4220 *Biochemistry* **2009,** *48,* 4220–4230
DOI:10.1021/bi900413g

BIOCHEMISTRY
including biophysical chemistry & molecular biology
*Current Topic*

# Molecular and Mechanistic Properties of the Membrane-Bound Mitochondrial Monoamine Oxidases[†]

Dale E. Edmondson,*[,‡] Claudia Binda,[§] Jin Wang,[‡] Anup K. Upadhyay,[‡] and Andrea Mattevi[§]

[‡]*Departments of Biochemistry and Chemistry, Emory University, Atlanta, Georgia 30322, and*
[§]*Department of Genetics and Microbiology, University of Pavia, via Ferrata 1, Pavia, 27100 Italy*

*Received March 10, 2009; Revised Manuscript Received April 9, 2009*

ABSTRACT: The past decade has brought major advances in our knowledge of the structures and mechanisms of MAO A and MAO B, which are pharmacological targets for specific inhibitors. In both enzymes, crystallographic and biochemical data show their respective C-terminal transmembrane helices anchor the enzymes to the outer mitochondrial membrane. Pulsed EPR data show both enzymes are dimeric in their membrane-bound forms with agreement between distances measured in their crystalline forms. Distances measured between active site-directed spin-labels in membrane preparations show excellent agreement with those estimated from crystallographic data. Our knowledge of requirements for development of specific reversible MAO B inhibitors is in a fairly mature status. Less is known regarding the structural requirements for highly specific reversible MAO A inhibitors. In spite of their 70% level of sequence identity and similarities of $C_\alpha$ folds, the two enzymes exhibit significant functional and structural differences that can be exploited in the ultimate goal of the development of highly specific inhibitors. This review summarizes the current structural and mechanistic information available that can be utilized in the development of future highly specific neuroprotectants and cardioprotectants.

The flavoenzymes monoamine oxidase A (MAO A)[1] and monoamine oxidase B (MAO B) have been extensively studied with approximately 20000 published papers listed in databases such as PubMed. This long-term interest stems from their roles in the oxidative catabolism of important amine neurotransmitters, including serotonin, dopamine, and epinephrine. Since the original discovery by Zeller (*1*) that hydrazines are MAO inhibitors that can lead to mood elevation, many pharmaceutical and academic laboratories have developed MAO inhibitors with potential clinical use; these include seven different MAO inhibitors approved by the Food and Drug Administration. The concept that humans and other mammals contain two distinct MAOs was a controversial topic until the demonstration (*2*) that MAO A and MAO B are encoded by separate genes that correspond to different amino acid sequences that are ~70% identical. All mammals contain both MAO A and MAO B, which are localized in the outer membrane of mitochondria in most tissues. It is currently believed that the respective genes encoding MAO A and MAO B evolved by a duplication event from a single ancestral gene. Teleost (fish) and lower invertebrates are found to contain only a single MAO gene. Limited studies of zebrafish MAO suggest the single MAO exhibits properties of both MAO A and of MAO B, although little is known regarding its specific enzymological and structural properties (*3*).

MAO A and MAO B catalyze the oxidative deamination of amine neurotransmitters using $O_2$ as the electron acceptor. Table 1 shows the relative rates of biological amine oxidation by MAO A and by MAO B. There are two general catalytic reaction pathways as shown in Scheme 1. For most substrates, both MAO A and MAO B follow the lower loop of the pathway shown in Scheme 1 in which oxygen reacts with the enzyme−product complex before product has dissociated. There is general consensus that the deprotonated (rather than the protonated) amine moiety on the substrate binds to the active site on the enzymes and is oxidized to the protonated imine (*4*) (found with both MAO B and MAO A) with the covalent 8α-*S*-cysteinyl FAD cofactor being reduced to its hydroquinone form. To complete the catalytic cycle, the reduced FAD cofactor reacts with $O_2$ to generate oxidized flavin and $H_2O_2$. The dissociated protonated imine is released from the enzyme and undergoes a noncatalyzed hydrolysis to form $NH_4^+$ and the corresponding aldehyde. The products of the MAO-catalyzed reactions (especially the $H_2O_2$) have sufficient deleterious reactivities to account for associated health-related problems. Therefore, considerable

[†]Support for much of the work cited in this review is from the National Institutes of Health (GM-29433) and is gratefully acknowledged. A.M. acknowledges grant support from Associazione Italiana per la Ricerca sul Cancro and the Cariplo foundation.

*To whom correspondence should be addressed: Department of Biochemistry, Emory University, 1510 Clifton Rd., Atlanta, GA 30322. Phone: (404) 727-5972. Fax: (404) 727-2738. E-mail: deedmon@emory.edu.

[1]Abbreviations: MAO A, monoamine oxidase A; MAO B, monoamine oxidase B; DEER, double electron−electron resonance; ENDOR, electron−nuclear double resonance; EPR, electron paramagnetic resonance; NMR, nuclear magnetic resonance; LSD-1, lysine-specific histone demethylase-1; SET, single electron transfer.

 Published on Web 4/16/2009 

Table 1: Turnover Numbers for the Oxidation of Naturally Occurring Amine Neurotransmitters by Purified Human MAO A and MAO B[a]

| | MAO A | | MAO B | |
|---|---|---|---|---|
| amine substrate | $k_{cat}$ ($min^{-1}$) | $K_m$ ($\mu$M) | $k_{cat}$ ($min^{-1}$) | $K_m$ ($\mu$M) |
| serotonin | 198 (183) | 295 ± 46 | 61 (33) | 2270 ± 310 |
| dopamine | 75 (71) | 240 ± 43 | 277 (65) | 128 ± 16 |
| histamine | $K_i$ = 2.1 mM[b] | | 3.5 (2.0)[c] | ~4000 |
| *N*-methylhistamine | $K_i$ > 15 mM[b] | | 35 (17) | 166 ± 8.1 |

[a] $k_{cat}$ values at saturating concentrations of organic substrate and of $O_2$. Values in parentheses are for saturating amine levels at air saturation. All data are determined following the rate of $O_2$ uptake polarographically. [b] Histamines are poorly oxidized by MAO A, and the $K_i$ values listed are competitive inhibition constants with kynuramine as the substrate. A histamine $k_{cat}$ value of 0.6 $min^{-1}$ is found, and *N*-methylhistamine is oxidized with a $k_{cat}$ value of ~0.1 $min^{-1}$. Both values were determined at saturating amine concentrations at air saturation. [c] Values determined at a substrate concentration of 5 mM.

Scheme 1: General Reaction Scheme for MAO Catalysis

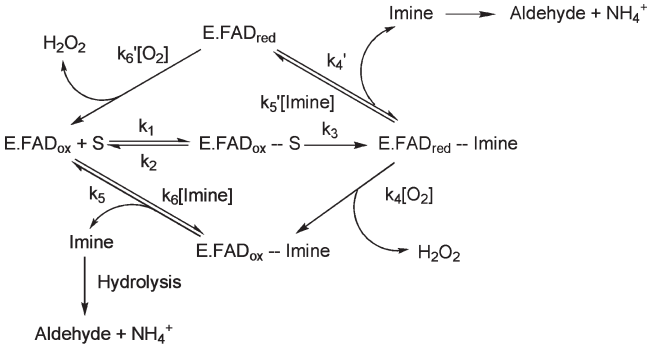


effort has gone into the design and development of specific MAO inhibitors that could function in a protective role. Since the original observation that MAO inhibition results in mood elevation, six (and a recent seventh) FDA-approved MAO inhibitors have been available for clinical use. The use of these compounds as pharmacological agents has declined because of the side effects, which require careful dietary restrictions to reduce the intake of biogenic amines in foods that could serve as false neurotransmitters. This review summarizes available knowledge of the molecular and catalytic properties of MAO A and MAO B relevant to current and future development of protective agents that could be effective in both neuro- and cardiotherapies.

## MEDICAL AND PHARMACOLOGICAL IMPORTANCE

*MAO B*. The observation by Fowler's laboratory (*5*) that MAO B levels in the human increase ~4−5-fold on aging had been observed earlier in rats and presents a rationale for the involvement of MAO B in age-related neurological disorders such as Parkinson's disease (*6*). Increased MAO B levels would be expected to diminish dopamine levels and to increase levels of the catalytic reaction products, dopanal and $H_2O_2$. Dopanal has been implicated in α-synuclein aggregation involved in the etiology of Parkinson's disease (*7*). Increased levels of $H_2O_2$ in the cell promote apoptotic signaling events, resulting in the decreased levels of dopamine-producing cells and the development of Parkinson's disease (*6*). A classic example of the MAO B-catalyzed bioactivation of a compound that

Scheme 2: Structures of MAO B-Specific Inhibitors

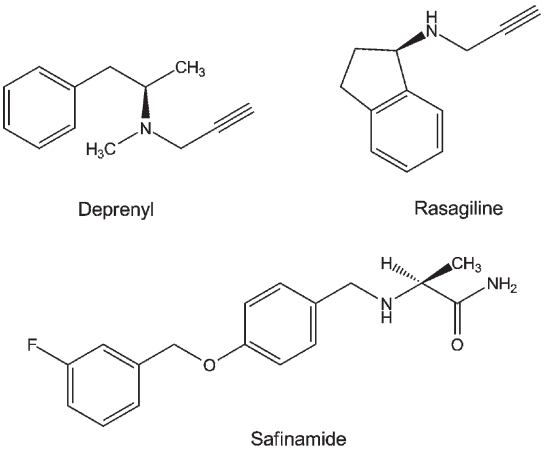


results in the genesis of Parkinson-like syndrome is the oxidation of MPTP to $MPP^+$ (*8*) which functions as a mitochondrial toxin and results in the destruction of glial cells in the *substantia nigra*. Inhibition of MAO B results in protection from this cell-destructive bioactivation.

Agents that specifically target the inhibition of MAO B are likely to serve as neuroprotectants. Indeed, treatment of pre-Parkinson's patients with deprenyl (and, more recently, with rasagiline) (see Scheme 2 for structures) has been shown to be effective in reducing the development (but not prevention) of the disease (*9*). Both of the above-mentioned inhibitors are acetylenic compounds that form covalent adducts with N(5) of the covalent FAD of MAO B and are pharmacologically inert as MAO A inhibitors. Recent results with safinamide (see Scheme 2 for the structure), a very specific MAO B noncovalent inhibitor, suggest it may function effectively as a neuroprotectant.

*MAO A*. MAO A functions specifically in the oxidative metabolism of serotonin, although it also oxidizes dopamine effectively. Complete elimination of MAO A activity by genetic deletion in mice (*10*) [and one case in humans (*11*)] results in the expression of aggressive behavior (*12*). Recent studies on MAO A knockout mice demonstrated a marked effect of higher serotonin levels on cardiac remodeling (*13*). MAO A levels have also been found to dramatically increase (~9-fold) in the heart of aged rats, thereby suggesting the probability of age-dependent increases in MAO A levels in humans (*14*). The consequence of this large increase in the level of MAO A in the heart is suggested to involve increased apoptosis and necrosis of cardiac cells due to increased levels of reactive oxygen species from the $H_2O_2$ produced. As suggested from the work of Parini and co-workers (*15*), the identification of the involvement of MAO A in cardiac cellular degeneration thus presents a potential drug target for the development of cardioprotective agents for an aging population. Initial attempts have been published (*16*); however, this area of MAO research is still in its infancy.

## MOLECULAR STRUCTURES OF HUMAN MAO B AND MAO A

*Expression and Purification*. Both MAO A and MAO B are known to be membrane-associated enzymes that are located specifically to the outer mitochondrial membrane. The purification of these enzymes, in the past, represented a formidable challenge since most mammalian tissues contained both enzymes that are not readily separable from one another due to their

molecular similarities. Prior to 1999, human MAO A was either purified from human placental tissue (required six or seven placentas for one enzyme purification in a 35% yield) (*17*) or purified from a *Saccharomyces cerevisiae* expression system (*18*) which required the growth of 20 L of culture to provide sufficient cells for isolation of a reasonable quantity (50−100 mg) of enzyme. During this same time period, the most convenient source of MAO B was bovine liver mitochondria (*19*).

The development of expression systems for human MAO B and MAO A provided a stable source of either enzyme and greatly facilitated both structural and mechanistic work. Procedures and conditions for the expression of human MAO B (*20*) and human MAO A (*21*) in the *Pichia pastoris* yeast system have been published. This system allows the purification of ~200 mg of pure enzyme from 2 L of fermentation medium and also allows incorporation of site-directed mutations on either enzyme as another tool for structure and mechanistic probes. Expressed full-length human MAO A or MAO B is situated in the outer mitochondrial membrane of the yeast cell and constitutes ~50% of the total protein content of mitochondrial outer membrane preparations. The availability of large quantities of homogeneous protein led to the determination of their structural properties of both enzymes by X-ray crystallography.

*Structures of Human MAO A and MAO B.* With the availability of reagent quantities of purified enzymes, the three-dimensional structures of human MAO B (*22*), human MAO A (*23*, *24*), and rat MAO A (*26*) have been determined and are shown as ribbon diagrams in Figure 1. The X-ray structure of human MAO B has been determined in complex with a range of inhibitors (see below) to a resolution of 1.65 Å for the best structure. Human and rat MAO A X-ray structures have been determined to 2.2 and 3.3 Å resolution, respectively. All of the enzymes have structures with similar folds and with a high degree of identity in their respective $C_\alpha$ coordinates. These structures show that the membrane binding motifs of the enzymes are located in the group of 35−40 C-terminal residues. In human MAO B, this transmembrane region folds into an α-helix protruding perpendicularly from the main globular body of the protein, although the last 20 residues of this motif are too disordered to provide definitive electron density (*22*). The C-terminal part of human MAO A has a topology similar to that of rat MAO A with the electron density sufficiently defined to provide a complete view of the transmembrane α-helix (*24*). These structural data support previous biochemical data (*29*) that identified the C-terminal helix as the mode of binding of MAO A or MAO B to the outer mitochondrial membrane. It is of interest that chimeric enzymes constructed using fragments of MAO A and MAO B show that "swaps" of the respective C-terminal helices between MAO B and MAO A result in inactive enzyme (*30*, *31*), suggesting that there are differences in the specific membrane binding architectures between the two isozymes.

The protein structures around the active site covalent FAD coenzymes are quite similar among the three known MAOs. The position of the FAD cofactor with respect to the overall structure is highly conserved, and the substrate-binding sites consist of elongated cavities (Figure 1) whose features will be thoroughly discussed in the next section. In all three enzymes, the flavin rings exist in "bent" rather than the more common planar configurations about the N(5)−N(10) axis (Figure 2), demonstrating strain at the coenzyme binding sites that may have catalytic relevance (see below). In all cases, the flavin side chains are in extended conformations, which is commonly observed in the structures of

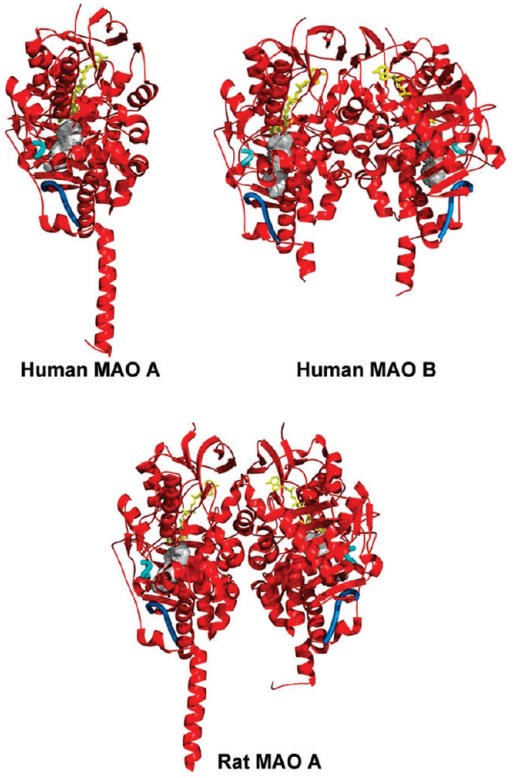


FIGURE 1: Ribbon diagram showing the three-dimensional structures of human MAO A (*24*), human MAO B (*25*), and rat MAO A (*26*). All structures are oriented with the C-terminal transmembrane helices pointing downward. The FAD cofactor is presented as yellow balls and sticks. The active site cavity in each enzyme molecule is drawn as a gray surface. The cavity-shaping loop (residues 210−216 in human and rat MAO A and residues 201−207 in human MAO B) is highlighted in cyan. The loop lining the entrance cavity space in human MAO B (residues 99−110) (*27*) is colored blue. The corresponding residues in rat and human MAO A adopt the same conformation. The cavities were calculated with VOIDOO (*28*) and the structural representations produced with Pymol (www.pymol.org).

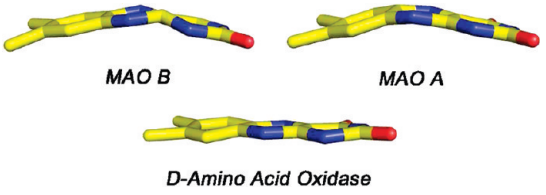


FIGURE 2: Relative conformations of the isoalloxazine rings of the 8α-*S*-cysteinylFAD coenzymes in human MAO B and MAO A (top). For the sake of comparison, the ring conformation of the FAD cofactor of *Rhodotorula gracilus* D-amino acid oxidase is also shown (below). These structures are taken from coordinates deposited in the Protein Data Bank as entries 1OJA, 2Z5X, and 1C0K, respectively.

other flavoenzymes containing FAD as a cofactor (*32*). Another example of strain about the FAD site is the finding in human MAO B (*27*) and in human MAO A (*24*) that the amide linkage between Cys397 (Cys406 in MAO A) (the site for the covalent flavin 8α-thioether linkage) and Tyr398 (Tyr407 in MAO A) is in a *cis* conformation.

The largest differences in structures among the three known structures of MAO are the respective natures of their oligomeric states (Figure 1); human MAO B and rat MAO A are dimers, while human MAO A is a monomer. A survey of the literature shows membrane proteins are generally oligomeric in the membrane, with dimerization being most common (*33*). Theoretical

modeling studies and species-dependent genetic analyses have led Andres et al. (*34*) to propose that the monomeric structure of human MAO A could be due to a human exclusive Glu151Lys mutation at a site located near the dimer interface. All other species of MAO A and MAO B have a conserved Glu at this position. The agreement of the experimental observation of a monomeric human MAO A structure with the prediction by Andres et al. (*34*) resulted in questions regarding the functional significance of this structural difference and whether the monomeric form of human MAO A existed in the membrane or whether it was an artifact of protein solubilization and purification from its membrane environment.

To address these questions, pulsed EPR (DEER) experiments were performed using a nitroxide spin-labeled pargyline analogue that was covalently attached to the FAD coenzyme in both MAO A and MAO B. This technique can measure distances between two paramagnetic species separated by distances of up to 60 Å and is applicable for detergent-solubilized as well as membrane preparations (*35*). This approach provides additional distance data for addressing the question of whether the enzyme structure determined by X-ray crystallography is the same as that in a membrane environment. Recently published pulsed EPR data show that all rat and human MAO A and MAO B enzymes are dimeric in their membrane-bound forms and that dimer formation is independent of whether Glu or Lys is at position 151 (or its analogous site) (*36*). In the detergent-solubilized, purified preparations, both human and rat MAO B are found to remain 100% dimeric, whereas human and rat MAO A exist only fractionally (50%) in their dimeric forms. Dissociation of oligomeric structures of membrane proteins in detergent micelles has precedent in the literature as reported for the bovine mitochondrial ADP/ATP carrier (*37*) and is found to also be the case for MAO A but not for MAO B. The human MAO A monomer species is more likely to crystallize than its dimeric form, while the dimer structure of rat MAO A is more readily crystallized. The similarities of DEER-measured distances (Figure 3) with those measured from crystallographic data of human MAO B and rat MAO A provide definitive evidence of the biological significance of their respective crystal structures.

*Structures of Active Site Cavities in MAO B and MAO A and Influence of Inhibitor Binding on Those Structures*. The structural elucidation of human and rat MAOs revealed that substrate binding and oxidation occurs in elongated cavities extending from the flavin site at the core of the enzyme to the surface of the protein on the opposite side of the FAD adenosine ring (Figures 1 and 4). Although in all three enzymes the cavities are generally hydrophobic, details of the active site architectures demonstrate differences in their respective structural properties that account for their distinct substrate and inhibitor specificities. The recently reported 2.2 Å crystal structure of human MAO A in complex with harmine (*24*) allows a more detailed comparison of the active sites between the two human enzymes (Figure 4, top panel). The volume of the human MAO A cavity is ~400 Å$^3$, whereas that of the two combined cavities of human MAO B is ~700 Å$^3$. The MAO B cavity is bipartite and is comprised of two separate spaces, the substrate cavity (~400 Å$^3$) and the entrance cavity (~300 Å$^3$), with the latter facing the solvent after movement of loop 99−110 (colored blue in Figure 1). Whether the active site of MAO B is a large single cavity or a bipartite cavity is an example of catalytic site plasticity determined by the conformation of Ile199. The side chain of this "gating" residue may, depending on the nature of the bound ligand, adopt two different conformations ("closed" and "open") (Figure 5) (*27*). The corresponding residue in human and in rat MAO A is Phe208, but it does not function as a gating residue. Mutagenesis experiments were performed on human MAO B Ile199Phe since the well-studied bovine enzyme contains a Phe at position 199 rather than an Ile (*38*). Structural and inhibitor binding experiments with this mutant form of human MAO B demonstrated that the bulky Phe side chain impedes such conformational flexibility, reduces the space of the entrance cavity, and interferes with the binding of MAO B-specific inhibitors (*38*). These findings provide a structural rationale for differential binding affinities reported in the literature on comparison of bovine and human MAO B preparations (*39*) and present a warning on pitfalls that can be encountered in the use of differing MAO sources for development of inhibitors of human MAO (*40*).

Another difference between MAO A and MAO B structures also involves the active site cavity structures. The Tyr326 side chain in MAO B, although not directly involved in the partition of the two cavities, does produce a restriction that is less pronounced in human MAO A where Ile335 occupies that position. Conserved active site residues in both enzymes include the Tyr pair of the aromatic sandwich (Figure 4) at the *re* face of

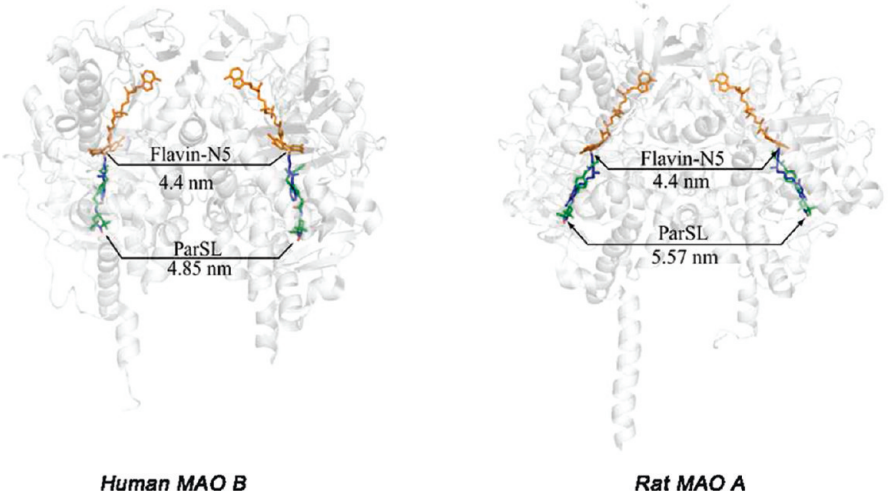


FIGURE 3: Distances calculated from X-ray structures and determined from analysis of DEER dipolar couplings between the flavin cofactors (orange) and between the pargyline analogue spin-labels (green). The positions of the pargyline spin-labels in each active site are based on superpositions with the known structures of pargyline covalent adducts (blue).

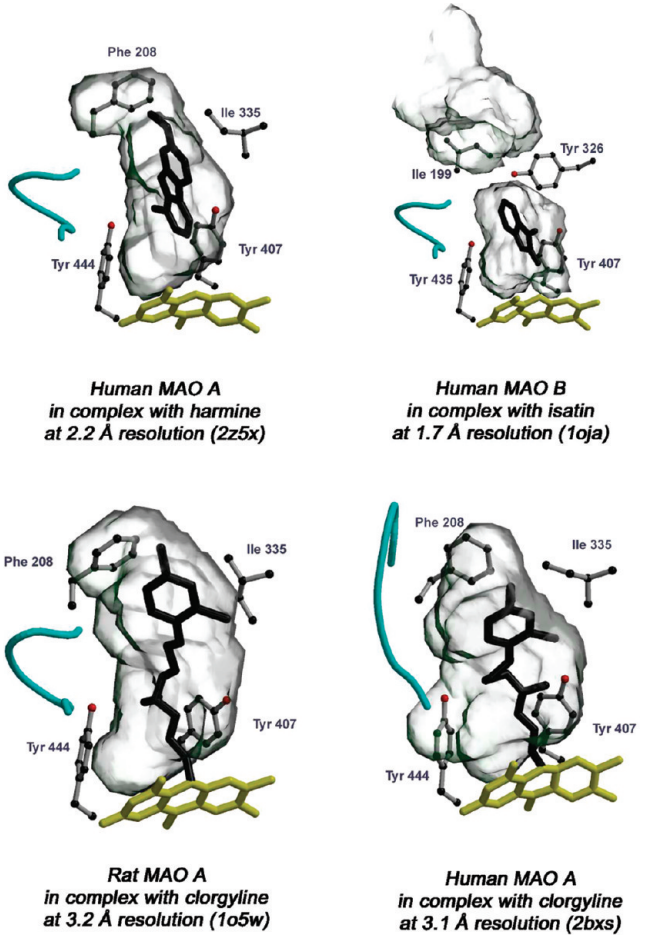


FIGURE 4: Active site cavity and inhibitor binding in MAO A and MAO B. The protein molecule is rotated approximately 180° with respect to the orientation of Figure 1 (i.e., with the C-terminal α-helix pointing upward). In the top panel, among the known structures of human MAO B in complex with various inhibitors (Figure 5), that with isatin (*27*) has been chosen to be compared with binding of harmine to human MAO A because they are both noncovalent inhibitors of similar size and binding affinity (MAO B−isatin $K_i$ = 3 $\mu$M; MAO A−harmine $K_i$ = 0.6 $\mu$M). In the bottom panel, the structures of human and rat MAO A in complex with clorgyline are compared. The flavin and inhibitor molecules are shown as yellow and black ball-and-stick representations, respectively. The Tyr side chains beside the flavin (Tyr407 and Tyr444 in MAO A and Tyr398 and Tyr435 in MAO B) form the conserved "aromatic sandwich" (*41*). Among the other active site residues, Phe208 (Ile199 in MAO B) and Ile335 (Tyr326 in MAO B) are drawn to highlight their role in determining substrate/inhibitor specificity between MAO A and MAO B (see the text). The Protein Data Bank entries for each structure are in parentheses. The cavity-shaping loop (residues 210−216 in MAO A) is colored cyan as in Figure 1. The cavities were calculated with VOIDOO (*28*), and the images were produced with Bobscript (*42*) and Raster3D (*43*).

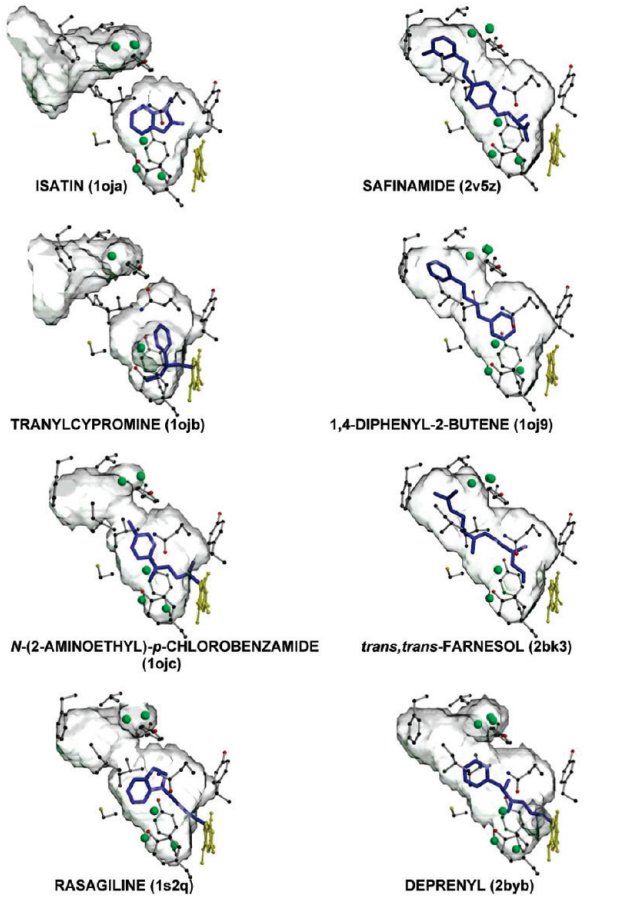


FIGURE 5: Comparison of active site cavity structures of human MAO B in different enzyme−inhibitor complexes. The Protein Data Bank entries for each structure are in parentheses. The protein molecule is rotated approximately 90° around an axis perpendicular to the plane of picture with respect to Figure 4. The residues lining the cavity are shown as gray ball-and-stick representations with carbon, oxygen, nitrogen, and sulfur atoms colored black, red, blue, and yellow, respectively. Water molecules included in the cavity are represented as green spheres. The flavin is colored yellow and the inhibitor molecule blue.

the flavin coenzyme isoalloxazine ring and a Lys residue hydrogen bonded via a water molecule to the N(5) position of the flavin (Lys305 in MAO A and Lys296 in MAO B). Other nonconserved residues in the active sites include Asn181 and Ile180 in MAO A (Cys172 and Leu171 in MAO B, respectively), which, however, do not significantly affect the shapes of the cavities. Therefore, the MAO A Phe208-Ile335 and MAO B Ile199-Tyr326 pairs appear to be major determinants in dictating the differential substrate and inhibitor specificities of the two enzymes.

An intriguing issue in MAO enzymology is to understand where and how the substrates (or inhibitors) are admitted to the active sites. In human MAO B, the cavity is extended and substrate binding is likely to occur in the proximity of the outer mitochondrial membrane surface region with the entrance loop (residues 99−110) involved in the access (colored blue in Figure 1). In both human and rat MAO A, the active site cavity is more compact. However, Son et al. (*24*) have recently demonstrated by site-directed mutagenesis that the conserved Gly110 is important for ensuring flexibility of the entrance loop required to provide access for the substrate. Therefore, the structural data suggest that MAO A and MAO B ligands follow similar pathways in binding. The cavity-shaping loop (residues 210−216 in MAO A, cyan in Figures 4 and 5) adopts a helical conformation that is conserved in all structures except for human MAO A in complex with clorgyline (Figure 4). This is unlikely to be due to the inhibitor because rat MAO A complexed with clorgyline retains the folded conformation of loop 210−216, although the inhibitor adopts a slightly different conformation. However, this observation suggests that this loop may be more susceptible to structural flexibility in MAO A than in MAO B.

The high-resolution crystal structures of human MAO B in complex with different inhibitors of clinical interest allow a more in-depth analysis of the active site cavity, which is important because of the pharmacological relevance of these enzymes. The elongated cavity of human MAO B is mostly hydrophobic, with

a small hydrophilic area in front of the *re* face of the flavin cofactor (*27*) that is occupied by highly conserved water molecules (Figure 5). Human MAO B can bind compounds of different sizes, and a number of them react with the flavin cofactor to form a covalent adduct (Figure 5), an example of the classical definition of a mechanism-based inhibitor. In general, all inhibitors contain an aromatic moiety (as expected considering the aromatic nature of the neurotransmitter substrates), but the cavity showed a significant affinity also for aliphatic ligands such as *trans*,*trans*-farnesol. Recent data show inhibition of MAO B by agents found in common laboratory plasticware; these include the slip agent, oleamide, and the biocide, di(2-hydroxyethyl)methyldodecylammonium ion (*44*). This inhibitory versatility is related to the plasticity of the human MAO B active site cavity. As described above, depending on the conformation of gating residue Ile199, the cavity can host either small inhibitors, such as isatin and tranylcypromine, or cavity-filling ligands such as safinamide, *trans*,*trans*-farnesol, and 1,4-diphenyl-2-butene (a component of polystyrene plasticware) (*45*). In the former case, the active site is restricted to a small cavity separated from an entrance cavity space that opens to the exterior like a funnel, whereas in the latter, the cavity shape is a compact ellipsoid (Figure 5). Binding of inhibitors such as rasagiline (*46*), *N*-(2-aminoethyl)-*p*-chlorobenzamide (*27*), and deprenyl (*23*) induces a midspan type of cavity because they are large enough to push gating residue Ile199 into the open conformation. With these inhibitors, the shape of the resulting cavity has a more bipartite character than that induced by the cavity-filling inhibitors. It is important to note that in all these MAO B−inhibitor complexes, the positions of the active site residues, apart from gating residue Ile199, are highly conserved, and this cavity plasticity is probably determined by subtle conformational changes. From a pharmacological viewpoint, this inhibitory versatility has important implications. Small compounds such as isatin and tranylcypromine, which can be hosted in a limited pocket, show similar binding affinities for both MAO A and MAO B, whereas cavity-filling ligands are highly specific MAO B inhibitors. Less self-explanatory are the inhibitory properties of rasagiline, which is highly specific for MAO B, although it occupies only one-half of the entire cavity (Figure 5). Even more surprising is the evidence that a rasagiline analogue methylated on the amino moiety of the propargyline chain connecting the inhibitor to the flavin loses this characteristic specificity for MAO B (*47*). Moreover, the covalent nature of some MAO inhibitors raises additional questions. What is the mechanism for covalent adduct formation of the propargyl moiety of compounds such as rasagiline or deprenyl with flavin? Unpublished work in this laboratory shows the reaction occurs without consumption of $O_2$, suggesting no catalytic turnover in the inhibition reaction.

Recent studies on the differential inhibition of MAO B and MAO A with the vinyl fluoro amine Mofegiline (*48*) show covalent adduct formation with the flavin in MAO B but only noncovalent competitive inhibition with MAO A. This inhibitor is one of the most effective MAO B active site inhibitors the authors have encountered. The proposed mechanism of inhibition is shown in Scheme 3, where the adduct formed is at N(5) of flavin with the vinyl side chain of the inhibitor with accompanying loss of $F^-$. This adduct exhibits unique spectral properties in that the absorption bands of the adduct resemble those of the oxidized flavin (*48*) rather than the "bleached" form generally found with flavins alkylated at the N(5) position (*49*). The proposed reason this compound does not react irreversibly with

Scheme 3: Proposed Mechanism for Mofegiline Inhibition of Human MAO B

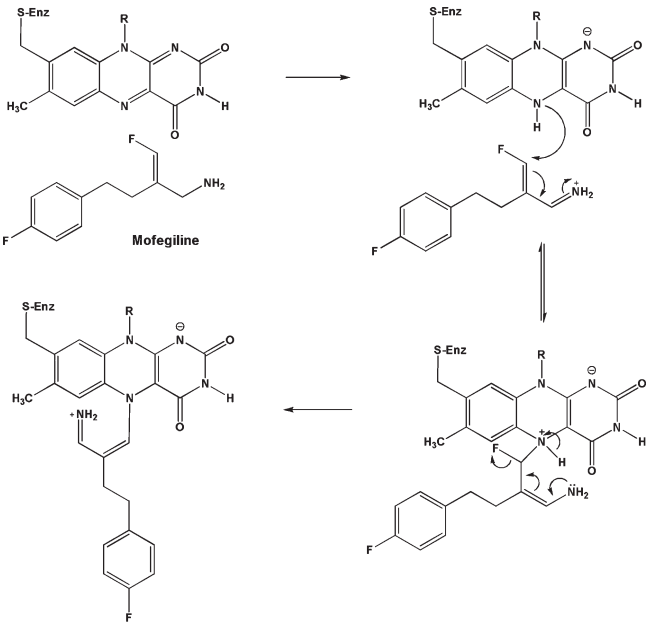


MAO A is that this enzyme is unable to oxidize arylalkylamine analogues with an extended side chain (*50*). α-C−H bond cleavage of the amine side chain of Mofegiline is required for formation of reduced flavin, which then reacts nucleophilically with the vinyl fluoride to form the covalent adduct.

To date, essentially all irreversible MAO inhibitors form N(5) flavin adducts. The only exception is the flavin C(4a) adduct formed on inhibition and ring opening of tranylcypromine with MAO B (*27*). Previous model system studies of phenylethylhydrazine inhibition of MAO A or MAO B suggested the alkylflavin to be a C(4a) adduct; however, recent structural and mechanistic studies show MAO inhibition to involve covalent addition to the flavin N(5) position (*49*). Structural data on tranylcypromine inhibition of other flavin-dependent amine oxidases such as lysine-specific histone demethylase 1 (*51*) show the ring-opened cyclopropyl moiety to be linked to the flavin at both the N(5) and C(4a) positions. Therefore, the possibility remains that the adduct observed in tranylcypromine-inhibited MAO B may have originated from the initial formation of an N(5) adduct with subsequent migration occurring during the time period required for crystallization of the enzyme. Previous model system studies with alkyl adducts of flavins that were produced via photoreaction with phenylacetates show that thermal isomerization occurs between N(5) and C(4a) (*52*), so the possible isomerization occurring in the amine oxidases remains a concern in addressing mechanistic studies.

*Differences in Active Site Cavity Accessibilities between Human MAO B and MAO A and Comparison with Rat Enzymes*. In spite of their high levels of sequence identity (>90%) and the general assumption that rat MAO A and MAO B are reasonable substitutes for the human enzymes in drug development studies, there have been a number of reports in the literature that the rat enzymes exhibit different affinities (*40*) relative to the human enzymes. Confirmation of these differences has been achieved in experiments designed to monitor similarities and differences between rat and human MAO A and MAO B. Using a spin-labeled pargyline analogue (*53*), the accessibility of the bound nitroxide in human MAO A is found to be

considerably higher (~10-fold) than that in human MAO B. Rat MAO A and MAO B exhibit similar accessibilities to a neutral paramagnetic probe at a level intermediate between those of the two human enzymes (*53*). These data support the observation of differing affinities for selected inhibitors published in the literature and also demonstrate structural and/or dynamic differences between rat and human enzymes either in their soluble, purified forms or in their membrane-bound forms. Therefore, a measure of caution is urged by investigators in the field in attempting to extrapolate detailed molecular data to humans from data collected in rats.

## MECHANISTIC STUDIES ON MAO CATALYSIS

*Analysis of the Different Proposed Mechanisms of C−H Bond Cleavage*. C−H bond cleavage reactions occur by three possible mechanisms: heterolytic hydride transfer, heterolytic $H^+$ abstraction (includes the proposed ammonium cation radical as well as the polar nucleophilic mechanism), and homolytic $H^\bullet$ abstraction (see Scheme 4). Of these possibilities, the two heterolytic reactions that have been proposed have resulted in a good deal of controversy about whether MAO catalysis follows a hydride mechanism as suggested for the amino acid oxidase and the alcohol oxidase classes of flavoenzymes. Hydrogen atom abstractions involving the flavin triplet state are known to occur; however, no convincing evidence of ground-state flavins in either model systems or flavoenzymes has been published. The stereochemistry of the hydrogen transfer step is well-documented to be the pro-*R* H of the substrate for both MAO A and MAO B (*54*, *55*). This property differs from the Cu-quinoprotein amine oxidases in which both *R* and *S* stereochemistry of hydrogen transfer is found (*56*). As is the case with the Cu-quinoprotein amine oxidases, MAO oxidation of benzylamines (*57*, *58*) and phenethylamines (*50*) exhibits large deuterium kinetic isotope effects showing, in most instances, that C−H bond cleavage is rate-limiting in catalysis. Previous studies of bovine MAO B have demonstrated that H tunneling contributes in the H transfer step (*59*). The evidence supporting a hydride transfer from substrate to flavin in other flavoprotein oxidases is suggested from $^{15}N$ kinetic isotope effect experiments (*60*, *61*). Other kinetic and structural data on the amino acid oxidases also support this mechanism (*62*). A strong argument against the hydride mechanism for MAO catalysis is the demonstration that either MAO A or MAO B readily oxidizes arylalkylhydrazines to form diazenes (*49*). It is difficult to envision the oxidation of a hydrazine to a diazene by abstraction of a hydride ion from a nitrogen atom. In fact, the amine oxidases appear to be unique among flavoenzymes in their ability to catalyze hydrazine oxidation reactions. The polar nucleophilic mechanism discussed below would be compatible with the oxidation of a hydrazine moiety.

Scheme 4: General Mechanisms for C−H Bond Cleavage Reactions in Flavoenzymes

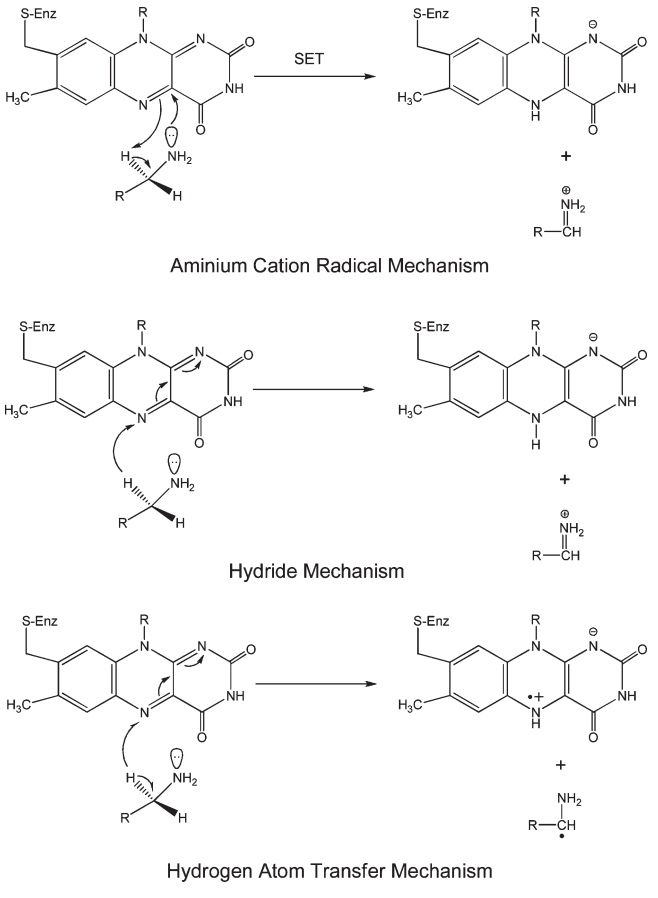


Similarities in high-field EPR and ENDOR spectral properties of the anionic FAD semiquinones of both human MAO A and yeast D-amino acid oxidase (*63*) indicate similar distributions of spin densities among their flavoenzyme semiquinones. The significance of these studies is to definitively rule out any flavin radical−tyrosyl radical equilibria in MAO A as suggested in a previous study (*64*) and thought to have implications for the radical mechanism. Recent work on a blue light sensor flavoprotein demonstrates that a tyrosyl radical adjacent to a neutral flavin radical (*65*) exhibits considerable spin coupling that is readily observed in X-band EPR spectra. Such spin coupling is not observed in MAO A, and this constitutes additional evidence that no tyrosyl radical is apparent in MAO A or MAO B. EPR and ENDOR studies of model flavin semiquinones and flavoenzyme semiquinones have long been known from the pioneering work of Ehrenberg and colleagues (*66*), and the spin distribution of the radical about the isoalloxazine ring in a number of flavoenzymes with different functions is found to be quite similar. Therefore, the spectral properties of flavoenzyme semiquinones do not provide definitive evidence to dictate whether they follow similar catalytic mechanisms.

Of the $H^+$ abstraction mechanistic pathways proposed, perhaps the aminium cation radical mechanism or SET mechanism proposed by Silverman and co-workers (*67*) has received the most attention. This mechanism is based on the premise that the $pK_a$ of α-CH protons of an amine requires a very strong base for abstraction that would not likely be fulfilled by a basic amino acid side chain. To lower the $pK_a$ values of these protons for $H^+$ abstraction by a basic amino acid residue, the amine is first oxidized to the amine cation radical form, which results in acidification of the α-CH group and thus allows $H^+$ abstraction. To date, experiments designed to test this mechanism have failed to provide supporting evidence that this mechanism is operational in MAO A or MAO B. No flavin radical intermediates are detected spectrally in stopped-flow experiments (*50*, *57*, *58*); no influence of magnetic field on the rate of enzyme reduction is observed (*68*), and the oxidation−reduction potential of the FAD cofactor is too low (~40 mV) (*69*) to be an effective oxidant of the deprotonated amine ($E_m$ = 1.5 V) (*70*). In addition to these mechanistic probes, the structures of MAO A and MAO B show no obvious basic amino acid residues that could serve as active site bases in catalysis. The main supporting evidence for the

Scheme 5: Reaction of Rimoldi's Amine with MAO B

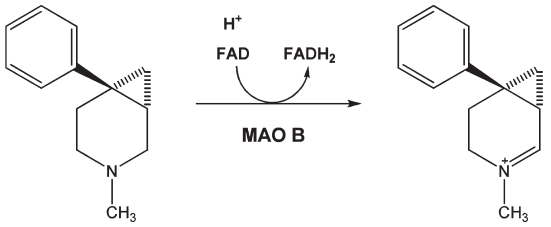


hemolytic one-electron mechanism is the observation that MAO A or MAO B is inactivated by cyclopropylamine analogues with subsequent ring opening, a reaction characteristic of radical reactions. Recent studies of the MAO B-catalyzed oxidation of "Rimoldi's Amine", which consists of a cyclopropyl group fused to an *N*-methylpyridinium ring, show the cyclic imine formation to occur without opening of the cyclopropyl ring (Scheme 5) (*71*) which would be expected if the reaction were to involve radical intermediates. In the aggregate, these studies do not support the concept that the mechanism of amine oxidation in MAO is initiated by a hemolytic single-electron transfer step.

Current mechanistic data do support the polar nucleophilic mechanism proposed by Miller and Edmondson (*58*) for human MAO A catalysis, which is based on the observation of a $\rho$ value of ~2 from analysis of Hammett plots of steady-state and rapid-reaction kinetic data on the oxidation of a series of para-substituted benzylamine analogues. This behavior is also exhibited by rat MAO A (*72*) as well as mutants of both human and rat MAO A and appears to be the most definitive evidence of the abstraction of the pro-*R* α-CH group as a $H^+$ as the mode of C−H bond cleavage. Previous data on the Cu-quinoprotein plasma amine oxidase with a series of para-substituted benzylamine analogues show a $\rho$ value of ~1.4 for C−H bond cleavage (*ref73*). As most investigators accept a proton abstraction mechanism from the Schiff base intermediate in the quinoprotein-catalyzed amine oxidation, one can suggest a similar type of $H^+$ abstraction mechanism for the flavin-dependent amine oxidation. To accomplish this difficult proton abstraction [the p$K_a$ for a benzyl hydrogen is ~25 (*74*)], no basic amino acid residues are in the catalytic site, and therefore, the flavin must be activated to become a strong base. This could be accomplished by C(4a) addition of the amine followed by or in conjunction with abstraction of the α-CH group by the resulting basic N(5), which is estimated to exhibit a p$K_a$ of ~25 from NMR studies of reduced flavin models (*75*). The reaction mechanism for this proposed reaction is shown in Scheme 6.

Since deprotonated amines do not appear to exhibit the nucleophilicity to readily add to the flavin C(4a) position in model systems and no direct evidence for a stable amine−flavin adduct has been found, one must examine factors in the enzyme that would facilitate this type of reaction. Structural data show the isoalloxazine ring of the flavin to exist in a conformation ~30° bent from planarity in the oxidized form of the enzyme (Figure 2). This bending has been shown by NMR studies of other flavoenzymes to result in C(4a) being more electrophilic and N(5) being more nucleophilic (*76*). In addition, the presence of two tyrosyl rings approximately perpendicular to the *re* face of the flavin demonstrates the amine moiety of the substrate must pass between them to approach the flavin. Results from our laboratory show that mutagenesis of Tyr435 in MAO B and the corresponding Tyr444 in MAO A results in a functional enzyme with lowered activity that has been correlated with dipole−dipole

Scheme 6: Proposed Polar Nucleophilic Mechanism for the Reductive Half-Reaction of MAO Catalysis

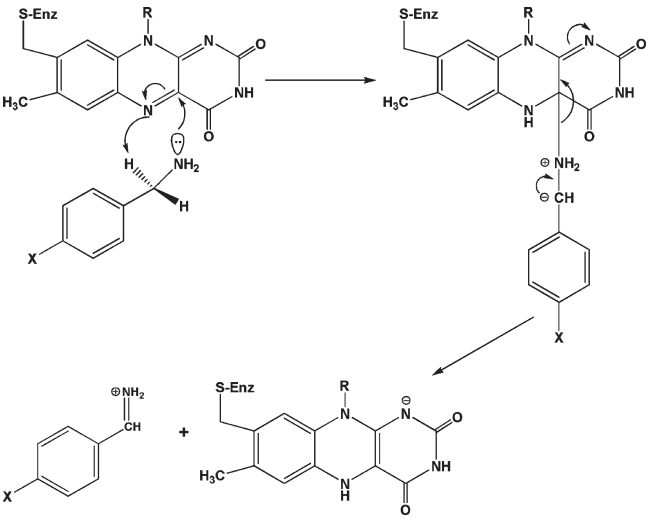


interactions of the phenolic ring and the deprotonated amine (*77*). This suggests that the combined dipole moments of the two tyrosyl residues would result in the distribution of the lone pair of electrons on the amine nitrogen to become more elongated, which would increase the effective nucleophilicity of the amine nitrogen. Both of the factors mentioned above would fit the proposed mechanism in Scheme 6.

In contrast to that of MAO A, analysis of the MAO B-catalyzed oxidation of a series of para-substituted benzylamine analogues shows the reaction rate to depend mainly on steric parameters with no detectable influence of substituent electronic effects (*57*). This behavior is suggested, by structural data, to reflect the steric constraints of the benzyl ring of the substrate in MAO B, which prevents the full expression of electronic parameters on the benzyl CH group (*58*). In contrast, the MAO A structure shows a more open and less restricted active site, which allows the substrate more steric freedom and therefore overlap of the $\pi$-orbitals for the full expression of para substituent electronic effects. In principle, alterations to the MAO B active site could decrease this proposed steric constraint, thereby allowing the expression of electronic effects on C−H bond cleavage. To date, such an approach has not been used.

The detailed mechanism of flavin-dependent amine oxidation remains a subject for additional studies. Not only is it important for the understanding of MAO A and MAO B catalysis, but it is also biologically important for our understanding of other amine oxidases such as LSD-1, the flavoenzyme involved in the epigenetic regulation of gene experession through histone demethylation (*51*).

*Reaction of MAO with $O_2$: The Oxidative Half-Reaction.* The second half-reaction of MAO A or MAO B catalysis is the oxidative half-reaction in which $O_2$ is reduced to $H_2O_2$ on reaction with the flavin hydroquinone. As discussed in the introductory section, the formation of $H_2O_2$ by MAO constitutes a potential source of toxic reactive oxygen species leading to apoptopic cellular responses. A key difference in the two forms is that the $K_m$ for $O_2$ with MAO B is ~240 $\mu$M (*57*) while the corresponding value for MAO A is ~12 $\mu$M (*78*). Thus, under normal cellular conditions, MAO A is operating at saturating concentrations of $O_2$ while MAO B is probably less than half saturated. The molecular basis for this difference is still unknown.

FIGURE 6: Location of three bound Xe atoms in the entrance cavity and substrate cavity of human MAO B (only one monomeric unit shown). Xenon is depicted as dark yellow spheres. FAD is colored yellow. The substrate binding domain is colored red, the FAD binding domain blue, and the membrane binding domain green. The substrate and entrance cavities of MAO B are colored cyan. Figure based on unpublished data from this laboratory.

Unpublished structural data show Xe (a proposed probe of $O_2$ binding sites in enzymes) to bind to MAO B both in the substrate cavity and in the entrance cavity (Figure 6). These data suggest the path by which $O_2$ approaches the reduced flavin is the entrance and substrate cavities in MAO B.

Stopped-flow experiments with bovine MAO B show that the reduced enzyme reacts with $O_2$ in a second-order manner with a rate constant of $3.6 \times 10^5$ $M^{-1}$ $min^{-1}$ that is 10-fold slower than that in which the imine product is still bound ($2 \times 10^6$ $M^{-1}$ $min^{-1}$) (*79*). This oxygen rate acceleration in the MAO byproduct is presumably due to the stabilizing effect of the protonated imine on the formation of superoxide anion (see below) in the first step of the oxygen reaction, analogous to the role of an active site histidine residue in glucose oxidase (*80*) (Scheme 7). Ramsay (*78*) has found that the MAO A rate of reaction with $O_2$ is accelerated by the presence of substrate to achieve a rate similar to that observed with MAO B. The reaction of reduced flavin coenzymes with $O_2$ is still an active area of investigation, especially among the flavoenzyme oxidase class where the reaction product is $H_2O_2$. From a structural point of view, both MAO A and MAO B contain lysine residues hydrogen bonded via an intervening $H_2O$ molecule to the N(5) position of their respective flavin coenzymes. This feature is also observed in the structures of a number of flavoenzyme oxidases. The mechanistic significance of this linkage has been suggested to be involved in the $O_2$ reaction (*81*).

It is now generally accepted that the reaction of triplet $O_2$ with singlet ground-state reduced flavin must involve a rate-limiting single electron transfer to form flavin semiquinone (the neutral form) and superoxide anion (*82*). This mechanism circumvents classical symmetry rules in such chemical reactions and has been investigated in detail with glucose oxidase (*80*). The reaction can

Scheme 7: Proposed Mechanisms for $O_2$ Reaction in the Oxidative Half-Reaction of MAO Catalysis

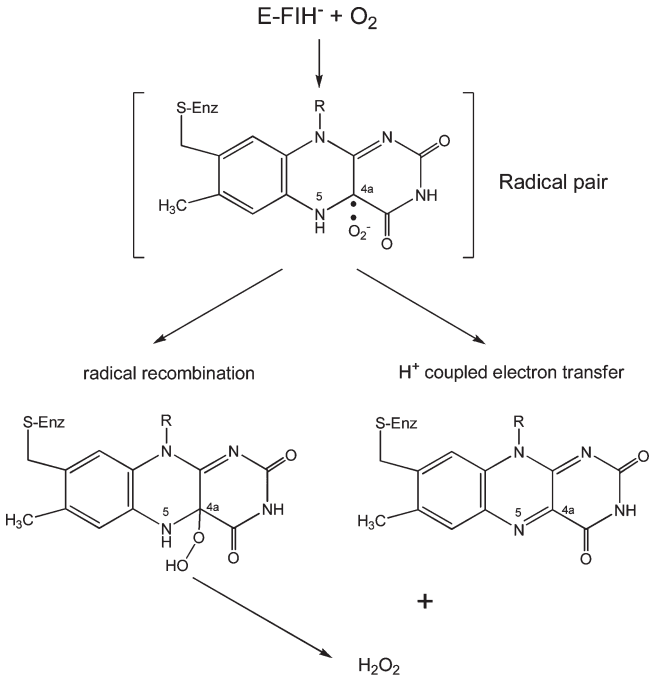


then proceed via two different mechanisms (Scheme 7). One is the recombination of the radical pair to form the C(4a) flavin peroxide which would subsequently release $H_2O_2$ and the oxidized coenzyme. This intermediate is formed in the flavoenzyme hydroxylase family (*83*) and has recently been observed in flavoenzyme oxidases (*84*, *85*). The other possibility is the reaction of superoxide with the flavin neutral radical to form $H_2O_2$ and oxidized flavin in a proton-coupled electron transfer step without an intermediate covalent linkage. Theoretical calculations for such a mechanism have been published (*81*), and recent experimental work on monomeric sarcosine oxidase supports these calculations. For example, mutagenesis of the $H_2O$-bonded lysine residue to the flavin results in a dramatic reduction in the rate of $O_2$ reoxidation of the reduced flavin (*86*). These results suggest that the reactions of MAO with $O_2$ will be vigorously investigated and will be important for fully explaining how these membrane-bound enzymes function in their oxidative half-reactions.

## ACKNOWLEDGMENT

We thank former colleagues, including Drs. P. Newton-Vinson, J. R. Miller, R. Nandigama, L. De Colibus, and M. Li, for their contributions to the project over the years. Ms. Milagros Aldeco has provided essential technical support for a major number of studies cited in this review. Finally, we acknowledge the contributions of the numerous collaborators who are cited in the references.

## REFERENCES

1. Zeller, E. A., and Bardsky, J. (1952) *In vivo* inhibition of liver and brain monoamine oxidase by 1-isonicotinyl-2-isopropyl hydrazine. *Proc. Soc. Exp. Biol. Med. 81*, 459–461.
2. Bach, A. W. J., Lan, N. C., Johnson, D. L., Abell, C. W., Bembenek, M. E., Kwan, S. W., Seeburg, P. H., and Shih, J. C. (1988) cDNA cloning of human liver monoamine oxidases A and B: Molecular basis of differences in enzymatic properties. *Proc. Natl. Acad. Sci. U.S.A. 85*, 4934–4938.

3. Setini, A., Pierucci, F., Senatori, O., and Nicotra, A. (2005) Molecular characterization of monoamine oxidase in zebrafish (*Danio rerio*). *Comp. Biochem. Physiol., Part B: Biochem. Mol. Biol. 140*, 153–161.
4. Edmondson, D. E., Bhattacharyya, A. K., and Walker, M. C. (1993) Spectral and kinetic studies of imine product formation in the oxidation of *p*-(N,N-dimethylamino)-benzylamine analogues by monoamine oxidase B. *Biochemistry 32*, 5196–5202.
5. Fowler, J. S., Logan, J., Volkow, N. D., Wang, G. J., MacGregor, R. R., and Ding, Y. S. (2002) Monoamine oxidase: Radiotracer development and human studies. *Methods 27*, 263–277.
6. Mallajosyula, J. K., Kaur, D., Chinta, S. J., Rajagopalan, S., Rane, A., Nicholls, D. G., Di Monte, D. A., Macarthur, H., and Andersen, J. K. (2008) MAO B elevation in mouse brain astrocytes results in Parkinson's pathology. *PloS One 3*, e1616.
7. Burke, W. J., Kumar, V. B., Pandey, N., Panneton, W. M., Gan, Q., Franko, M. W., O'Dell, M., Li, S. W., Pan, Y., Chung, H. D., and Galvin, J. E. (2008) Aggregation of α-synuclein by DOPAL, the monoamine oxidase metabolite of dopamine. *Acta Neuropathol. 115*, 193–203.
8. Jenner, P., and Marsden, C. D. (1988) MPTP-induced Parkinsonism as an experimental model of Parkinson's Disease. In *Parkinson's Disease and Movement Disorders* (Jankovic, J., and Tolosa, E., Eds.) pp 37−48, Urban & Schwarzenberg, Baltimore.
9. Chen, J. J., and Swope, D. M. (2007) Pharmacotherapy for Parkinson's disease. *Pharmacotherapy 27*, 161S–173S.
10. Cases, O., Seif, I., Grimsby, J., Gasper, P., Chen, K., Muller, U., Aguet, M., Babinet, C., Shih, J. C., and De Maeyer, E. (1995) Aggressive behavior and altered amounts of brain serotonin and norepinephrine in mice lacking MAO A. *Science 268*, 1763–1766.
11. Brunner, H. G., Nelen, M. R., van Zandvoort, N. G., Abeling, N. G. G. M., van Gennip, A. H., Wolters, E. C., Kuiper, M. A., Rogers, H. H., and van Oost, B. A. (1993) X-Linked borderline mental retardation with prominent behavioral disturbance: Phenotype, genetic localization, and evidence for disturbed monoamine metabolism. *Am. J. Hum. Genet. 52*, 1032–1039.
12. McDermott, R., Tingley, D., Cowden, J., Frazetto, G., and Johnson, D. D. P. (2009) Monoamine oxidase A gene (MAO A) predicts behavioral aggression following provocation. *Proc. Natl. Acad. Sci. U.S.A. 106*, 2118–2123.
13. Lairez, O., Calise, D., Bianchi, P., Ordener, C., Spreux-Varoquaux, O., Guilbeau-Frugier, C., Escourrou, G., Seif, I., Roncalli, J., Pizzinat, N., Galinier, M., Parini, A., and Mialet-Perez, J. (2009) Genetic deletion of MAO-A promotes serotonin-dependent ventricular hypertrophy by pressure overload. *J. Mol. Cell. Cardiol.,* in press.
14. Maurel, A., Hernandez, C., Kunduzova, O., Bompart, G., Cambon, C., Parini, A., and Francés, B. (2003) Age-dependent increase in hydrogen peroxide production by cardiac monoamine oxidase A in rats. *Am. J. Physiol. 284*, H1460–H1467.
15. Bianchi, P., Kunduzova, O., Masini, E., Cambon, C., Bani, D., Raimondi, L., Seguelas, M. H., Nistri, S., Colucci, W., Leducq, N., and Parini, A. (2005) Oxidative stress by monoamine oxidase mediates receptor-independent cardiomyocyte apoptosis by serotonin and postischemic myocardial injury. *Circulation 112*, 3297–3305.
16. Gentili, F., Pizzinat, N., Ordener, C., Marchal-Victorion, S., Maurel, A., Hofmann, R., Renard, P., DeLagrange, P., Pigini, M., Parini, A., and Giannella, M. (2006) 3-[5-(4,5-Dihydro-1H-imidazol-2-yl)-furan-2-yl]phenylamine (amifuraline), a promising reversible and selective peripheral MAO-A inhibitor. *J. Med. Chem. 49*, 5578–5586.
17. Weyler, W., and Salach, J. I. (1985) Purification and properties of mitochondrial monoamine oxidase type A from human placenta. *J. Biol. Chem. 260*, 13199–13207.
18. Weyler, W., Titlow, C. C., and Salach, J. I. (1990) Catalytically active monoamine oxidase type A from human liver expressed in *Saccharomyces cerevisiae* contains covalent FAD. *Biochem. Biophys. Res. Commun. 173*, 1205–1211.
19. Salach, J. I. (1979) Monoamine oxidase from beef liver mitochondria: Simplified isolation procedure, properties, and determination of its cysteinyl flavin content. *Arch. Biochem. Biophys. 192*, 128–137.
20. Newton-Vinson, P., Hubálek, F., and Edmondson, D. E. (2000) High-level expression of human liver monoamine oxidase B in *Pichia pastoris*. *Protein Expression Purif. 20*, 334–345.
21. Li, M., Hubálek, F., Newton-Vinson, P., and Edmondson, D. E. (2002) High-level expression of human liver monoamine oxidase A in *Pichia pastoris*: Comparison with the enzyme expressed in *Saccharomyes cerevisae*. *Protein Expression Purif. 24*, 152–162.
22. Binda, C., Newton-Vinson, P., Hubálek, F., Edmondson, D. E., and Mattevi, A. (2002) Structure of human monoamine oxidase B, a drug target for the treatment of neurological disorders. *Nat. Struct. Biol. 9*, 22–26.
23. De Colibus, L., Li, M., Binda, C., Lustig, A., Edmondson, D. E., and Mattevi, A. (2005) Three-dimensional structure of human monoamine oxidase A (MAO A): Relation to the structures of rat MAO A and human MAO B. *Proc. Natl. Acad. Sci. U.S.A. 102*, 12684–12689.
24. Son, S. Y., Ma, J., Kondou, Y., Yoshimura, M., Yamashita, E., and Tsukihara, T. (2008) Structure of human monoamine oxidase A at 2.2-Å resolution: The control of opening the entry for substrates/inhibitors. *Proc. Natl. Acad. Sci. U.S.A. 105*, 5739–5744.
25. Binda, C., Wang, J., Pisani, L., Caccia, C., Carotti, A., Salvati, P., Edmondson, D. E., and Mattevi, A. (2007) Structures of human monoamine oxidase B complexes with selective noncovalent inhibitors: Safinamide and coumarin analogs. *J. Med. Chem. 50*, 5848–5852.
26. Ma, J., Yoshimura, M., Yamashita, E., Nakagawa, A., Ito, A., and Tsukihara, T. (2004) Structure of rat monoamine oxidase A and its specific recognitions for substrates and inhibitors. *J. Mol. Biol. 338*, 103–114.
27. Binda, C., Li, M., Hubálek, F., Restelli, N., Edmondson, D. E., and Mattevi, A. (2003) Insights into the mode of inhibition of human mitochondrial monoamine oxidase B from high resolution crystal structures. *Proc. Natl. Acad. Sci. U.S.A. 100*, 9750–9755.
28. Kleywegt, G. J., and Jones, T. A. (1994) Detection, delineation, measurement and display of cavities in macromolecular structures. *Acta Crystallogr. D50*, 178–185.
29. Mitoma, J., and Ito, A. (1992) Mitochondrial targeting signal of rat liver monoamine oxidase B is located at its carboxy terminus. *J. Biochem. 111*, 20–24.
30. Chen, K., Wu, H. F., and Shih, J. C. (1996) Influence of C terminus on monoamine oxidase A and B catalytic activity. *J. Neurochem. 66*, 797–803.
31. Gottowik, J., Malherbe, P., Lang, G., Da Prada, M., and Cesura, A. M. (1995) Structure/function relationships of mitochondrial monoamine oxidase A and B chimeric forms. *Eur. J. Biochem. 230*, 934–942.
32. De Colibus, L., and Mattevi, A. (2006) New frontiers in structural flavoenzymology. *Curr. Opin. Struct. Biol. 16*, 722–728.
33. Sachs, J. N., and Engelman, D. M. (2006) Introduction to the membrane protein reviews: The interplay of structure, dynamics, and environment in membrane protein function. *Annu. Rev. Biochem. 75*, 707–712.
34. Andres, A. M., Soldevila, M., Navarro, A., Kidd, K. K., Olivia, B., and Bertranpetit, J. (2004) Positive selection in MAO A gene is human exclusive: Determination of the putative amino acid change selective in the human lineage. *Hum. Genet. 115*, 377–386.
35. Fajer, P. G., Brown, L., and Song, L. (2007) Practical Pulsed Dipolar ESR (DEER). In *ESR spectroscopy in membrane biophysics* (Hemminga, M. A., and Berliner, L. J., Eds.) pp 95−128, Springer, New York..
36. Upadhyay, A. K., Borbat, P. P., Wang, J., Freed, J. H., and Edmondson, D. E. (2008) Determination of the oligomeric states of human and rat monoamine oxidase in the outer mitochondrial membrane and octyl-β-D-glucopyranoside micelles using pulsed dipolar electron spin resonance spectroscopy. *Biochemistry 47*, 1554–1566.
37. Kunji, E. R. S., and Harding, M. (2003) Projection structure of atractyloside-inhibited mitochondrial ADP/ATP carrier of *Saccharomyces cerevisiae*. *J. Biol. Chem. 278*, 36985–36988.
38. Hubálek, F., Binda, C., Khalil, A., Li, M., Mattevi, A., Castagnoli, N., and Edmondson, D. E. (2005) Demonstration of isoleucine 199 as a structural determinant for the selective inhibition of human monoamine oxidase B by specific reversible inhibitors. *J. Biol. Chem. 280*, 15761–15766.
39. Krueger, M. J., Mazouz, F., Ramsay, R. R., Milcent, R., and Singer, T. P. (1995) Dramatic species differences in the susceptibility of monoamine oxidase B to a group of powerful inhibitors. *Biochem. Biophys. Res. Commun. 206*, 556–562.
40. Navaroli, L., Daina, A., Favre, E., Bravo, J., Carotti, A., Leonetti, F., Catto, M., Carrupt, P. A., and Reist, M. (2006) Impact of species-dependent differences on screening, design, and development of MAO B inhibitors. *J. Med. Chem. 49*, 6264–6272.
41. Binda, C., Mattevi, A., and Edmondson, D. E. (2002) Structure-function relationships in flavoenzyme-dependent amine oxidations: A comparison of polyamine oxidase and monoamine oxidase. *J. Biol. Chem. 277*, 23973–23976.
42. Esnouf, R. M. (1999) Further additions to molScript version 1.4, including reading and contouring of electron-density maps. *Acta Crystallogr. D55*, 938–940.
43. Merritt, E. A., and Bacon, D. J. (1997) Raster3D: Photorealistic molecular graphics. *Methods Enzymol. 277*, 505–524.

44. McDonald, G. R., Hudson, A. L., Dunn, S. M. J., You, H. T., Baker, G. B., Whittal, R. M., Martin, J. W., Jha, A., Edmondson, D. E., and Holt, A. (2008) Bioactive contaminants leach from disposable laboratory plasticware. *Science 322*, 917.
45. Hubálek, F., Binda, C., Li, M., Mattevi, A., and Edmondson, D. E. (2003) Polystyrene microbridges used in sitting drop crystallization release 1,4-diphenyl-2-butene, a novel inhibitor of human MAO B. *Acta Crystallogr. D59*, 1874–1876.
46. Hubálek, F., Binda, C., Li, M., Herzig, Y., Sterling, J., Youdim, M. B., Mattevi, A., and Edmondson, D. E. (2004) Inactivation of purified human recombinant monoamine oxidases A and B by rasagiline and its analogues. *J. Med. Chem. 47*, 1760–1766.
47. Binda, C., Hubálek, F., Li, M., Herzig, Y., Sterling, J., Edmondson, D. E., and Mattevi, A. (2005) Binding of rasagiline-related inhibitors to human monoamine oxidases: A kinetic and crystallographic analysis. *J. Med. Chem. 48*, 8148–8154.
48. Milczek, E. M., Bonivento, D., Binda, C., Mattevi, A., McDonald I. A., and Edmondson, D. E. (2008) Structural and mechanistic studies of mofegiline inhibition of recombinant human monoamine oxidase B. *J. Med. Chem. 51*, 8019–8026.
49. Binda, C., Wang, J., Li, M., Hubálek, F., Mattevi, A., and Edmondson, D. E. (2008) Structural and mechanistic studies of arylalkylhydrazine inhibition of human monoamine oxidases A and B. *Biochemistry 47*, 5616–5625.
50. Nandigama, R. K., and Edmondson, D. E. (2000) Structure-activity relations in the oxidation of phenethylamine analogues by recombinant human liver monoamine oxidase A. *Biochemistry 39*, 15258–15265.
51. Yang, M. J., Culhane, J. C., Szewczuk, L. M., Jalili, P., Ball, H. L., Machius, M., Cole, P. A., and Yu, H. T. (2007) Structural basis for the inhibition of the LSD1 histone demethylase by the antidepressant trans-2-phenylcyclopropylamine. *Biochemistry 46*, 8058–8065.
52. Walker, W. H., Hemmerich, P., and Massey, V. (1967) Reductive photoalkylation of flavin nucleus and flavin catalyzed photodecarboxylation of phenylacetate. *Helv. Chim. Acta 50*, 2269–2279.
53. Upadhyay, A. K., Wang, J., and Edmondson, D. E. (2008) Comparison of the structural properties of the active site cavities of human and rat monoamine oxidases A and B in their soluble and membrane-bound forms. *Biochemistry 47*, 526–536.
54. Yu, P. H., Bailey, B. A., Durden, D. A., and Boulton, A. A. (1986) Stereospecific deuterium substitution at the α-carbon position of dopamine and its effect on oxidative deamination catalyzed by MAO A and MAO B from different tissues. *Biochem. Pharmacol. 35*, 1027–1036.
55. Li, M. (2006) Comparative mechanistic and structural approaches to investigate the membrane-bound enzymes monoamine oxidase A and monoamine oxidase B. Ph.D. Dissertation, Emory University, Atlanta.
56. Farnum, M. F., and Klinman, J. P. (1986) Stereochemical probes of bovine plasma amine oxidase: Evidence for mirror-image processing and a *syn* abstraction of hydrogens from C-1 and C-2 of dopamine. *Biochemistry 25*, 6028–6036.
57. Walker, M. C., and Edmondson, D. E. (1994) Structure-activity relationships in the oxidation of benzylamine analogues by bovine liver monoamine oxidase B. *Biochemistry 33*, 7088–7098.
58. Miller, J. R., and Edmondson, D. E. (1999) Structure-activity relationships in the oxidation of *para*-substituted benzylamine analogues by recombinant human liver monoamine oxidase A. *Biochemistry 38*, 13670–13683.
59. Jonsson, T., Edmondson, D. E., and Klinman, J. P. (1994) Hydrogen tunneling in the flavoenzyme monoamine oxidase B. *Biochemistry 33*, 14871–14878.
60. Kurtz, K. A., Rishavy, M. A., Cleland, W. W., and Fitzpatrick, P. F. (2000) Nitrogen isotope effects as probes of the mechanism of D-amino acid oxidase. *J. Am. Chem. Soc. 122*, 12896–12897.
61. Ralph, E. C., Hirschi, J. S., Anderson, M. A., Cleland, W. W., Singleton, D. A., and Fitzpatrick, P. F. (2007) Insights into the mechanism of flavoprotein-catalyzed amine oxidation from nitrogen isotope effects on the reaction of N-methyltryptophan oxidase. *Biochemistry 46*, 7655–7664.
62. Harris, C. M., Pollegioni, L., and Ghisla, S. (2001) pH and kinetic isotope effects in D-amino acid oxidase catalysis: Evidence for a concerted mechanism in substrate dehydrogenation via hydride transfer. *Eur. J. Biochem. 268*, 5504–5520.
63. Kay, C. W. M., El Mkami, H., Molla, G., Pollegioni, L., and Ramsay, R. R. (2007) Characterization of the covalently bound anionic flavin radical in monoamine oxidase A by electron paramagnetic resonance. *J. Am. Chem. Soc. 129*, 16091–16097.
64. Rigby, S. E. J., Hynson, R. M., Ramsay, R. R., Munro, A. W., and Scrutton, N. (2005) A stable tyrosyl radical in monoamine oxidase A. *J. Biol. Chem. 280*, 4627–4631.
65. Nagai, H., Fukushima, Y., Okajima, K., Ikeuchi, M., and Mino, H. (2008) Formation of interacting spins on flavosemiquinone and tyrosyl radical in photoreaction of a blue light sensor BLUF protein TePixD. *Biochemistry 47*, 12574–12582.
66. Ehrenberg, A., Eriksson, L. E. G., and Hyde, J. S. (1971) Electron-nuclear double resonance from radicals of flavins and flavoproteins. In *Flavins and Flavoproteins* (Kamin, H., Ed.) pp 141−152, University Park Press, Baltimore.
67. Lu, X., Rodriguez, M., Ji, H., Silverman, R., Vintem, A. P. B., and Ramsay, R. R. (2002) Irreversible inactivation of mitochondrial monoamine oxidases. In *Flavins and Flavoproteins* (Chapman, S., Perham, R., and Scrutton, N., Eds.) pp 817−830, University Park Press, Baltimore.
68. Miller, J. R., Edmondson, D. E., and Grissom, C. B. (1995) Mechanistic probes of monoamine oxidase B catalysis: Rapid-scan stopped-flow and magnetic field independence of the reductive half reaction *J. Am. Chem. Soc. 117*, 7830–7831.
69. Newton-Vinson, P., and Edmondson, D. E. (1999) High-level expression, structural, kinetic, and redox characterization of recombinant human liver monoamine oxidase B. In *Flavins and Flavoproteins* (Ghisla, S., Kroneck, P., Macheroux, P., and Sund, H., Eds.) pp 431−438, Agency for Scientific Publications, Berlin.
70. Hull, L. A., Davis, G. T., Rosenblatt, D. H., and Mann, C. K. (1969) Oxidation of amines: Chemical and electrochemical correlations *J. Phys. Chem. 73*, 1389–1393.
71. Bissel, P., Khalil, A., Rimoldi, J. M., Igarashi, K., Edmondson, D. E., Miller, A., and Castagnoli, N. (2008) Stereochemical studies on the novel monoamine oxidase B substrates (1R,6S)- and (1S,6R)-3-methyl-6-phenyl-3-aza-bicyclo[4.1.0]heptane. *Bioorg. Med. Chem. 16*, 3557–3564.
72. Wang, J., and Edmondson, D. E. (2007) Do monomeric vs dimeric forms of MAO A make a difference? Comparison of the catalytic properties of rat and human MAO A's. *J. Neural Transm. 114* 721–724.
73. Hartmann, C., and Klinman, J. P. (1991) Structure-function studies of substrate oxidation by bovine serum amine oxidase: Relationship to cofactor structure and function. *Biochemistry 30*, 4605–4611.
74. Bordwell, F. G., Cheng, J. P., Satish, A. V., and Twyman, C. L. (1992) Acidities and homolytic bond dissociation energies (BDE's) of benzyl-type C-H binds in sterically congested substrates. *J. Org. Chem. 57*, 6542–6546.
75. Macheroux, P., Ghisla, S., Sanner, C., Rüterjans, H., and Müller, F. (2005) Reduced flavin: NMR investigations of N(5)-H exchange mechanism, estimation of ionization constants and assessment of properties as biological catalyst. *BMC Biochem. 6*, 26.
76. Eisenreich, W., Kemter, K., Bacher, A., Mulrooney, S. B., Williams, C. H., and Müller, F. (2004) $^{13}$C-, $^{15}$N-, and $^{31}$P-NMR studies of oxidized and reduced low mass thioredoxin reductase and some mutant proteins. *Eur. J. Biochem. 271*, 1437–1452.
77. Li, M., Binda, C., Mattevi, A., and Edmondson, D. E. (2006) Functional role of the "aromatic cage" in human monoamine oxidase B: Structures and catalytic properties of Tyr435 mutant proteins. *Biochemistry 45*, 4775–4784.
78. Ramsay, R. R. (1991) Kinetic mechanism of monoamine oxidase A. *Biochemistry 30*, 4624–4629.
79. Husain, M., Edmondson, D. E., and Singer, T. P. (1982) Kinetic studies on the catalytic mechanism of liver monoamine oxidase. *Biochemistry 21*, 595–600.
80. Roth, J. P., and Klinman, J. P. (2003) Catalysis of electron transfer during activation of $O_2$ by the flavoprotein glucose oxidase. *Proc. Natl. Acad. Sci. U.S.A. 100*, 62–67.
81. Prabhakar, R., Li, M., Musaev, D. G., Morokuma, K., and Edmondson, D. E. (2005) A density functional theory (DFT) study of the spin forbidden dioxygen activation in monoamine oxidase B (MAO B). In *Flavins and Flavoproteins* (Nishino, T., Riura, R., Tanokura, M., and Fukui, K., Eds.) pp 127−131, ArchiTect, Inc., Tokyo.
82. Bruice, T. C. (1984) Oxygen-flavin chemistry. *Isr. J. Chem. 24*, 54–61.
83. Massey, V. (1994) Activation of molecular oxygen by flavins and flavoproteins. *J. Biol. Chem. 269*, 22459–22462.
84. Sucharitakul, J., Prongjit, M., Haltrich, D., and Chaiyen, P. (2008) Detection of a C(4a)-hydroperoxyflavin intermediate in the reaction of a flavoprotein oxidase. *Biochemistry 47*, 8485–8490.
85. Orville, A. M., Lountos, G. T., Finnegan, S., Gadda, G., and Prabhakar, R. (2009) Crystallographic, spectroscopic and computational analysis of a flavin C(4a)-oxygen adduct in choline oxidase. *Biochemistry 48*, 720–728.
86. Zhao, G. H., Bruckner, R. C., and Jorns, M. S. (2008) Identification of the oxygen activation site in monomeric sarcosine oxidase: Role of Lys265 in catalysis. *Biochemistry 47*, 9124–9135.